Treating singularities present in the Sutcliffe-Tennyson vibrational Hamiltonian in orthogonal internal coordinates

Gábor Czakó
Department of Theoretical Chemistry, Eötvös University, H-1518 Budapest 112, P.O. Box 32, Hungary

Viktor Szalay
Crystal Physics Laboratory, Research Institute for Solid State Physics and Optics, Hungarian Academy of Sciences, P.O. Box 49, H-1525 Budapest, Hungary

Attila G. Császár and Tibor Furtenbacher
Department of Theoretical Chemistry, Eötvös University, H-1518 Budapest 112, P.O. Box 32, Hungary

(Received 30 September 2004; accepted 11 October 2004; published online 16 December 2004)

Two methods are developed, when solving the related time-independent Schrödinger equation (TISE), to cope with the singular terms of the vibrational kinetic energy operator of a triatomic molecule given in orthogonal internal coordinates. The first method provides a mathematically correct treatment of all singular terms. The vibrational eigenfunctions are approximated by linear combinations of functions of a three-dimensional nondirect-product basis, where basis functions are formed by coupling Bessel-DVR functions, where DVR stands for discrete variable representation, depending on distance-type coordinates and Legendre polynomials depending on angle bending. In the second method one of the singular terms related to a distance-type coordinate, deemed to be unimportant for spectroscopic applications, is given no special treatment. Here the basis set is obtained by taking the direct product of a one-dimensional DVR basis with a two-dimensional nondirect-product basis, the latter formed by coupling Bessel-DVR functions and Legendre polynomials. With the basis functions defined, matrix representations of the TISE are set up and solved numerically to obtain the vibrational energy levels of H_3^+. The numerical calculations show that the first method treating all singularities is computationally inefficient, while the second method treating properly only the singularities having physical importance is quite efficient. © *2005 American Institute of Physics.* [DOI: 10.1063/1.1827594]

I. INTRODUCTION

During the last three decades several solution strategies were proposed and related codes developed for the accurate computation of rovibrational energy levels of small molecules,[1] sometimes up to the dissociation limit(s). The most efficient codes seem to employ variants of the discrete variable representation (DVR) technique[2–7] and the related quadrature approximation,[4,8,9] and for triatomic species the use of the Sutcliffe-Tennyson rovibrational Hamiltonian[10] has become widespread.[8,11] Strategies and codes applicable for the four-,[12–16] five-,[17–19] and six-atomic[20] (ro)vibrational problems have appeared. Nevertheless, accurate computation of rovibrational states of triatomic molecules still provides a challenge when singularities in the Hamiltonian come into play.[6]

Singularities will always be present in an internal coordinate rovibrational Hamiltonian expressed in the moving body-fixed frame.[21] Theoretical techniques that do not treat the singularities in the rovibrational Hamiltonian may result in sizeable errors for some of the higher-lying rovibrational wave functions, which have significant amplitude at the singularities. Radial singularities in the Hamiltonian become relevant especially for X_3 species among triatomic molecules but they may lead to eigenvalue convergence problems in other, larger species, as well. We note in this respect that Gottfried, McCall, and Oka[22] recently measured transitions from energy levels of the H_3^+ molecular ion above the barrier to linearity, when the isosceles equilibrium geometry of H_3^+ is flattened by insertion of one of the hydrogens into a H_2 unit, present on the ground electronic state at about 10 000 cm^{-1} above the ground vibrational level. These high-energy experimental transitions provide a critical test of purely *ab initio* techniques employed for their calculation, as a preliminary analysis by Gottfried, McCall, and Oka[22] indicated.

Apart from approaches which avoid the introduction of certain singularities during construction of the Hamiltonian,[23–26] i.e., *a priori*, we are aware of only a few *a posteriori* strategies to cope with singular terms in rovibrational Hamiltonians when solving the related time-independent Schrödinger equation by means of (nearly) variational techniques.

Henderson, Tennyson, and Sutcliffe[27] combined a direct-product basis with an analytic formula to calculate the matrix elements of the R_2^{-2} part of the kinetic energy operator [see Eq. (1) below] by using spherical oscillator functions[28] and extra transformations. Using this algorithm *all* the bound vibrational states of H_3^+ have been calculated successfully.

Watson[29] employed an artificial wall of $10^{+6}\,cm^{-1}$ for undesired linear and nonphysical regions of the potential en-

ergy surface (PES) in his calculations, based on three Morse coordinates corresponding to H–H bonds, on H_3^+. This procedure did not work above the barrier to linearity; consequently, Watson advocated the use of hyperspherical coordinates to avoid the radial singularity problem.

Bramley *et al.*[30] (BTCC) employed an efficient technique treating the radial singularity by using two-dimensional nondirect-product basis functions, which are the analytic eigenfunctions of the spherical harmonic oscillator Hamiltonian,[31] which includes a harmonic R^2 potential. After the R_2^2 potential was added to the kinetic energy operator, the matrix elements of the R_2- and Θ-dependent part of the kinetic energy operator [see again Eq. (1) below] could be calculated analytically resulting in a diagonal finite basis representation (FBR) matrix. Consequently, the R_2^2 potential had to be subtracted from the potential energy. The potential energy with the harmonic $-R_2^2$ term had only diagonal nonzero matrix elements in the R_1 DVR but off-diagonal nonzero elements in the (R_2,Θ) FBR, which were calculated by using the quadrature approximation.

Instead of the nondirect-product FBR/DVR approach of BTCC, Mandelshtam and Taylor[32] advocated a simple and efficient direct-product DVR procedure made suitable to treat the singularity numerically by symmetrization of the sinc-DVR basis employed and use of an angular momentum cutoff.

A simple and efficient regularization technique advocated by Baye and co-workers[33] can also be employed to treat terms singular in the Hamiltonian during grid-based variational calculations. This approach has been employed to treat the radial singularities present in triatomic rovibrational Hamiltonians.[34]

In this paper we describe a FBR strategy based on the use of Bessel-DVR functions, developed recently by Littlejohn and Cargo,[35] and several resulting implementations for coping with the radial singularity present, for example, in the Sutcliffe-Tennyson triatomic vibrational Hamiltonian expressed in orthogonal internal coordinates.[10] A concise overview of discrete Bessel representations was published by Lemoine[36] in 2003, making their detailed discussion in this paper unnecessary.

After the Introduction we describe in Sec. II what type of singularities are present in the Sutcliffe-Tennyson triatomic vibrational Hamiltonian expressed in orthogonal internal coordinates and how we propose to treat the radial singularity if it becomes important during solution of the related time-independent Schrödinger equation. In Sec. III an implementation of a possible FBR method using three-dimensional nondirect-product basis in orthogonal Radau or Jacobi coordinate systems is discussed. The potential energy matrix is set up employing two different FBRs. In Sec. IV an efficient algorithm is described, whereby the singularity problem is solved in the Jacobi coordinate system by using a two-dimensional nondirect-product basis. The paper is ended with Conclusions (Sec. V).

II. SINGULARITIES IN THE SUTCLIFFE-TENNYSON TRIATOMIC VIBRATIONAL HAMILTONIAN IN ORTHOGONAL COORDINATES

In the Sutcliffe-Tennyson Hamiltonian[10] the vibrational kinetic energy operator of a triatomic molecule in the orthogonal Jacobi[37] or Radau[38] coordinates (R_1,R_2,Θ) is written in atomic units as

$$\hat{K}=-\frac{1}{2\mu_1}\frac{\partial^2}{\partial R_1^2}-\frac{1}{2\mu_2}\frac{\partial^2}{\partial R_2^2}-\left(\frac{1}{2\mu_1 R_1^2}+\frac{1}{2\mu_2 R_2^2}\right)\times\left(\frac{\partial^2}{\partial\Theta^2}+\cot\Theta\frac{\partial}{\partial\Theta}\right), \tag{1}$$

where μ_1 and μ_2 are appropriately defined mass-dependent constants,[10] and the volume element of integration is $dR_1dR_2d(\cos\Theta)$. In a mathematical sense $\hat{K}$ has three singularities, at $R_1=0$, at $R_2=0$, and at $\sin\Theta=0$. The Θ-dependent part of Eq. (1) is always singular if the molecule vibrates to the linear geometry or, in a more technical sense, if the basis functions sample the linear geometry.

A solution strategy of the bending singularity problem is offered by the differential equation

$$-\left(\frac{\partial^2}{\partial\Theta^2}+\cot\Theta\frac{\partial}{\partial\Theta}\right)P_\ell(\cos\Theta)=\ell(\ell+1)P_\ell(\cos\Theta), \tag{2}$$

where the analytic eigenfunctions $\{P_\ell(\cos\Theta)\}_{\ell=0}^{L-1}$ are the classical orthogonal Legendre polynomials. Therefore, Legendre polynomials are especially suitable basis functions for solving the bending singularity problem and most of the variational (ro)vibrational programs indeed use Legendre-DVR basis[39] for describing angle-bending motions.

In most cases the radial (stretching-type) singularities present in Eq. (1) may be ignored because the value of the potential energy function is very high and the wave function is going to vanish when the R_1 or R_2 coordinates closely approach or are equal to zero. In the case of the H_3^+ molecular ion, however, one must solve the radial singularity problem as linear geometries, arising from the insertion of the third H into a bond between two Hs, are sampled at relatively low energies. Clearly, one cannot use the quadrature approximation for computing the matrix elements of the R_1^{-2} and R_2^{-2} operators when they become singular.

To move forward let us consider the matrix representation of $\hat{K}$ using Legendre polynomials

$$\langle P_\ell|\hat{K}|P_{\ell'}\rangle=\hat{K}_{R_1,\ell}\delta_{\ell,\ell'}+\hat{K}_{R_2,\ell}\delta_{\ell,\ell'}, \tag{3}$$

where

$$\hat{K}_{R_j,\ell}=-\frac{1}{2\mu_j}\frac{\partial^2}{\partial R_j^2}+\frac{1}{2\mu_j R_j^2}\ell(\ell+1) \tag{4}$$

and $j=1$ or 2. The Bessel-DVR functions developed recently by Littlejohn and Cargo,[35]

$$\left\{F_{\nu n_j}(R_j)=(-1)^{n_j+1}\frac{k_{j\nu}z_{\nu n_j}\sqrt{2R_j}}{(k_{j\nu}R_j)^2-z_{\nu n_j}^2}J_\nu(k_{j\nu}R_j)\right\}_{n_j=0}^{N_j-1},$$

where $\nu=\ell+1/2$ and $z_{\nu n_j}$ are the zeros of the Bessel functions $J_\nu(z)$, are suitable to solve the radial singularity problem as the matrix elements of the $\hat{K}_{R_j,\ell}$ operators can be evaluated using a simple analytical formula[35]

$$(\mathbf{K}_{R_j,\ell})_{n_j,n_j'}=\langle F_{\nu n_j}|\hat{K}_{R_j,\ell}|F_{\nu n_j'}\rangle$$
$$=\delta_{n_j,n_j'}\frac{1}{2\mu_j}\frac{k_{j\nu}^2}{3}\left[1+\frac{2\left[\left(\ell+\frac{1}{2}\right)^2-1\right]}{z_{\nu n_j}^2}\right]$$
$$+(1-\delta_{n_j,n_j'})\frac{1}{2\mu_j}(-1)^{n_j-n_j'}$$
$$\times 8k_{j\nu}^2\frac{z_{\nu n_j}z_{\nu n_j'}}{(z_{\nu n_j}^2-z_{\nu n_j'}^2)^2}. \quad (5)$$

The radial grid points can be obtained as $r_{\nu_j n_j}=z_{\nu n_j}/k_{j\nu}$, where $k_{j\nu}=z_{\nu N_j}/R_{j\nu}^{\max}$; therefore, all the N_j grid points are in the interval $0<r_{\nu_j n_j}\leqslant R_{j\nu}^{\max}$.

III. FULL TREATMENTS OF SINGULARITIES IN ORTHOGONAL COORDINATE SYSTEMS

The three-dimensional nondirect-product basis $\{F_{\nu n_1}(R_1)F_{\nu n_2}(R_2)P_\ell(\cos\Theta)\}_{n_1,n_2,\ell=0}^{N_1-1,N_2-1,L-1}$, where $\nu=\ell+1/2$, can be used for solving the singularity problems both in the Jacobi and the Radau coordinate systems. Using a FBR, the sparse kinetic energy matrix can be obtained analytically as

$$(\mathbf{K}^{\mathrm{FBR}})_{n_1n_2\ell,n_1',n_2'\ell'}$$
$$=(\mathbf{K}_{R_1,\ell})_{n_1,n_1'}\delta_{n_2,n_2'}\delta_{\ell,\ell'}+\delta_{n_1,n_1'}(\mathbf{K}_{R_2,\ell})_{n_2,n_2'}\delta_{\ell,\ell'}. \quad (6)$$

The matrix representation of the potential energy operator $\hat{V}(R_1,R_2,\cos\Theta)$ can be set up via different FBR methods.[6] One can use N_1N_2L basis functions and the corresponding $(N_1L)(N_2L)L$ quadrature points, i.e., retaining all radial quadrature points corresponding to all possible values of ℓ, $\{r_{\nu_1n_1}\}_{\ell_1,n_1=0}^{L-1,N_1-1}\otimes\{r_{\nu_2n_2}\}_{\ell_2,n_2=0}^{L-1,N_2-1}\otimes\{q_\ell\}_{\ell=1}^{L}$, where ν_1 and ν_2 are $\ell_1+1/2$ and $\ell_2+1/2$, respectively, and the q_ℓs are the zeros of $P_L(\cos\Theta)$. Therefore, a $N_1N_2L\times N_1N_2L^3$-dimensional matrix $\boldsymbol{\mathcal{F}}$ can be set up as

$$\mathcal{F}_{\nu'n_1'n_2'\ell',\nu_1n_1\nu_2n_2\ell}$$
$$=w_{\nu_1n_1}^{1/2}w_{\nu_2n_2}^{1/2}w_\ell^{1/2}F_{\nu'n_1'}(r_{\nu_1n_1})F_{\nu'n_2'}(r_{\nu_2n_2})P_{\ell'}(q_\ell), \quad (7)$$

where $w_{\nu_1n_1}$, $w_{\nu_2n_2}$, and w_ℓ are the quadrature weights corresponding to the $r_{\nu_1n_1}$, $r_{\nu_2n_2}$, and q_ℓ grid points, respectively. It is straightforward to calculate the function values of the Legendre polynomials $P_{\ell'}(\cos\Theta)$ at the q_ℓ quadrature points. One can set up the **Q** coordinate matrix with matrix elements $Q_{\ell,\ell'}=\langle P_\ell(\cos\Theta)|\cos\Theta|P_{\ell'}(\cos\Theta)\rangle$, and the quadrature points $\{q_\ell\}_{\ell=1}^{L}$ are the eigenvalues of the **Q** matrix, while the **T** transformation matrix is defined by the eigenvectors of the **Q** matrix. The elements of the **T** matrix are $T_{\ell',\ell}=w_\ell^{1/2}P_{\ell'}(q_\ell)$, where the w_ℓs are the Gaussian quadrature weights. Calculation of the function values of the normalized Bessel-DVR basis $F_{\nu'n_j'}(R_j)$ at the $r_{\nu_jn_j}$ radial grid points is more involved. First one needs to determine the zeros of the $J_{\nu'}(z)$ Bessel functions, and then compute the radial grid points $r_{\nu_jn_j}$. When $\nu'\neq\nu_j$ in $F_{\nu'n_j'}(r_{\nu_jn_j})$, one has to calculate the function values of the Bessel functions $J_{\nu'}(k_{j\nu'}r_{\nu_jn_j})$. In the case of $\nu'=\nu_j$ the function values of the normalized Bessel-DVR basis functions are $F_{\nu'n_j'}(r_{\nu'n_j})=(-1)^{n_j'+1}\sqrt{k_{j\nu'}z_{\nu'n_j'}/2}\,J_{\nu'}'(z_{\nu'n_j'})\,\delta_{n_j',n_j}$, where the required function values of the Bessel derivative functions $J_{\nu'}'(z_{\nu'n_j'})$ can be obtained by using $J_{\nu'}'(z_{\nu'n_j'})=J_{\nu'-1}(z_{\nu'n_j'})$.

A FBR for the matrix representation of the Schrödinger equation of the Hamiltonian can be written as

$$\mathbf{HC}=(\mathbf{K}+\mathbf{V}^{\mathrm{FBR}})\mathbf{C}=(\mathbf{K}+\mathbf{S}^{-d}\boldsymbol{\mathcal{F}}\mathbf{V}^{\mathrm{diag}}\boldsymbol{\mathcal{F}}^{+}\mathbf{S}^{d-1})\mathbf{C}=\mathbf{CE}, \quad (8)$$

where $\mathbf{S}=\boldsymbol{\mathcal{F}}\boldsymbol{\mathcal{F}}^{+}$, $\boldsymbol{d}$ is a real number, the diagonal **E** and the **C** matrices contain the eigenvalues and eigenvectors of the Hamiltonian matrix (**H**), respectively, and

$$V^{\mathrm{diag}}_{\nu_1n_1\nu_2n_2\ell,\nu_1'n_1'\nu_2'n_2'\ell'}$$
$$=V(r_{\nu_1n_1},r_{\nu_2n_2},q_\ell)\,\delta_{\nu_1n_1\nu_2n_2\ell,\nu_1'n_1'\nu_2'n_2'\ell'}. \quad (9)$$

Equation (8) remains valid if one employs more quadrature points than the number of basis functions. In this case $\mathbf{V}^{\mathrm{FBR}}$ and consequently the eigenvalues become dependent on the weight functions. In all the computations reported the weights $w_{\nu_1n_1}=1$ and $w_{\nu_2n_2}=1$ were employed.

One can set up different FBRs varying parameter d in Eq. (8). Setting $d=1$ and $d=1/2$ an asymmetric[6] (AS-FBR) and a symmetric[2] (S-FBR) representation can be defined, respectively. Using the AS-FBR the $N_1N_2LN_1N_2L$-dimensional potential energy matrix becomes *asymmetric*. The advantage of this representation is twofold: (a) AS-FBR corresponds to the optimal-generalized DVR,[6] which is the most accurate generalized DVR method; and (b) when AS-FBR is employed with the same number of basis functions and quadrature points $\mathbf{V}^{\mathrm{FBR}}$ and the eigenvalues of the Hamiltonian will not depend on the weights.

Two algorithms were programmed. In both cases Eq. (6) was employed for the calculation of the kinetic energy matrix [**K** in Eq. (8)] elements, while either AS-FBR [$d=1$ in Eq. (8)] or S-FBR [$d=1/2$ in Eq. (8)] was used for setting up the matrix of the potential energy.

The numerical results, on the example of the H_3^+ molecular ion employing the PES of Polyansky *et al.*,[40] are presented in Table I. The vibrational eigenenergies (VE) have also been calculated by a standard DVR technique termed DOPI (DVR—Hamiltonian in orthogonal (O) coordinates—direct product (P) basis—iterative (I) sparse Lanczos eigensolver),[11,12] which employs analytic formulas[39] and the quadrature approximation during calculation of the kinetic energy matrix elements. While this PES is not the most accurate available for H_3^+, it has the distinct advantage that its dissociative behavior is correct, thus numerical results em-

TABLE I. Zero-point energy and the first 13 vibrational eigenenergies of H_3^+, in cm^{-1}, computed by the full FBR treatment of the singularities as described in Sec. III. The PES of H_3^+ is taken from Ref. 40 with the minimum at $r_e(HH)=1.649\,99$ bohrs. $m(H)=1.007\,537\,2u$ is used during all the computations. The number of basis functions is given as $(N_1\,N_2\,L)$, where N_1, N_2, and L denote the number of the R_1-, R_2-, and Θ-dependent functions, respectively. The radial grid points are in the intervals $0<r_{\nu_1 n_1}\leqslant 3.5+[0.001(\nu_1+1/2)]$ and $0<r_{\nu_2 n_2}\leqslant 3.0+[0.001(\nu_2+1/2)]$, all in bohr. Without symmetry analysis of the wave function or symmetrization of the basis functions no proper symmetry labels can be attached to the degenerate levels; therefore, these labels are omitted here. The zero-point energy of H_3^+ is the first entry of this table. All other eigenenergies refer to this energy.

	(10 10 10)		(16 16 16)		
Symmetry	AS-FBR[a]	S-FBR[b]	AS-FBR[a]	S-FBR[b]	Accurate[c]
A_1	4375.95	4375.94	4362.30	4362.30	4362.30
E	2449.29	2449.32	2521.19	2521.19	2521.19
E	2569.12	2569.03	2521.20	2521.20	2521.19
A_1	3232.63	3232.53	3179.21	3179.21	3179.20
A_1	4854.15	4854.17	4777.66	4777.66	4777.63
E	4893.82	4893.67	4997.61	4997.61	4997.60
E	5135.71	5135.61	4997.64	4997.64	4997.60
E	5492.34	5492.40	5554.82	5554.82	5554.82
E	5723.98	5723.28	5554.93	5554.93	5554.82
A_1	6432.95	6432.48	6263.94	6263.94	6263.85
E	6577.50	6577.58	7005.02	7005.02	7005.00
E	7253.74	7252.94	7005.24	7005.24	7005.00
A_1	7265.72	7265.79	7284.71	7284.71	7284.60
A_2	7613.55	7613.64	7492.57	7492.57	7492.53

[a]See text for the definition of AS-FBR.
[b]See text for the definition of S-FBR.
[c]Converged results obtained by the DOPI algorithm (Ref. 11), where the number of basis functions is (30 30 30) and the R_1 and R_2 Hermite-DVR grid points are in the intervals [0.9,3.5] and [0.05,2.95] bohr, respectively.

ploying quadrature points far from equilibrium are not subject to imprecision. The vibrational calculations have been carried out employing the Jacobi coordinate system. Note that although these coordinates do not carry the full symmetry of H_3^+, which possesses S_3 permutational symmetry, this in itself causes no difficulty in obtaining an accurate vibrational eigenspectrum of H_3^+, though it clearly hinders symmetry classification of the eigenstates.

In all cases studied the two different representations have been found to yield almost identical VEs,[41] independently of the convergence of the solution. This can be explained by the use of $N_1N_2L^3$ quadrature points, much higher than the number of basis functions, N_1N_2L. It must also be noted that the computation of the potential energy matrix needs a large amount of CPU time. To wit, a relatively small computation, e.g., with $N_1=N_2=L=16$, when even the lowest-lying VBOs are only quasiconverged, needs several days of CPU time on an average personal computer.[42] Therefore, this mathematically rigorous FBR treatment of the singularity problem proves to be computationally unfeasible.

IV. AN EFFICIENT ALGORITHM IN JACOBI COORDINATES

In the Jacobi coordinate system, where R_1 represents a diatomic distance and R_2 the separation of the third atom from the center of the mass of the diatom, the $R_1=0$ singularity will not occur in physically relevant cases because the potential energy value is going to be infinite and the wave function is going to vanish near nuclear coalescense points. Therefore, in the Jacobi coordinate system one can use a two-dimensional $\{R_2,\Theta\}$ nondirect-product basis for treating the remaining radial singularity, as was done, for example, by BTCC.[30] The full three-dimensional basis can be given by $\{\chi_{n_1}(R_1)F_{\nu n_2}(R_2)P_\ell(\cos\Theta)\}_{n_1,n_2,\ell=0}^{N_1-1,N_2-1,L-1}$, where $\{\chi_{n_1}(R_1)\}_{n_1=0}^{N_1-1}$ is a one-dimensional DVR basis (e.g., Hermite-DVR basis). One can obtain the matrix elements of the corresponding differential operator,

$$(\mathbf{K}_{R_1})_{n_1,n_1'}=\langle\chi_{n_1}(R_1)|-\frac{1}{2\mu_1}\frac{\partial^2}{\partial R_1^2}|\chi_{n_1'}(R_1)\rangle, \tag{10}$$

using exact analytical formulas.[39] The DVR representation of the R_1^{-2} part of the kinetic energy operator matrix $(\mathbf{R}_1^{-2})_{n_1,n_1'}=\langle\chi_{n_1}(R_1)|1/(2\mu_1R_1^2)|\chi_{n_1'}(R_1)\rangle$ can be calculated using the quadrature approximation

$$(\mathbf{R}_1^{-2})_{n_1,n_1'}=\frac{1}{2\mu_1 r_{n_1}^2}\delta_{n_1,n_1'}. \tag{11}$$

In the case of a Hermite-DVR basis, employed in the calculations reported in this paper,

$$r_{n_1}=\frac{q_{n_1}}{q_{N_1}}\frac{R_1^{\max}-R_1^{\min}}{2}+\frac{R_1^{\max}+R_1^{\min}}{2}, \tag{12}$$

where q_{n_1}s are the appropriate Gaussian quadrature points. Consequently, all grid points are defined in the interval $[R_1^{\min},R_1^{\max}]$. This way one can ensure that all grid points are in a physically meaningful region.

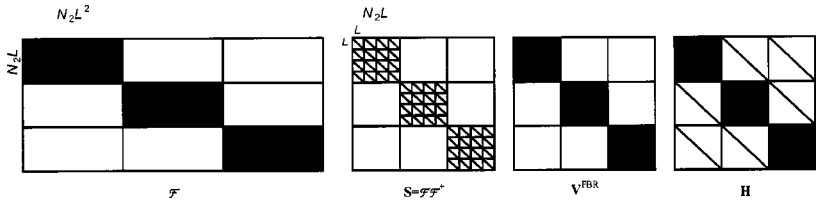

FIG. 1. Pictorial representation of the shape and the nonzero elements of the matrices $\boldsymbol{\mathcal{F}}$ [Eq. (14)], **S** [Eq. (8)], $\mathbf{V}^{\mathrm{FBR}}$ [Eq. (8)], and **H** [Eq. (8)] relevant for the algorithm described in Sec. IV (note that in this figure $N_1=3$ and $N_2=4$ and that the black boxes of $\boldsymbol{\mathcal{F}}$ also have some zero elements).

Finally, using Eqs. (5), (10), and (11) the DVR/FBR representation of the kinetic energy operator can be calculated by

$$(\mathbf{K}^{\mathrm{DVR/FBR}})_{n_1 n_2 \ell, n_1' n_2' \ell'} = (\mathbf{K}_{R_1})_{n_1,n_1'}\delta_{n_2,n_2'}\delta_{\ell,\ell'} + (\mathbf{R}_1^{-2})_{n_1,n_1'}\delta_{n_2,n_2'}\ell(\ell+1)\delta_{\ell,\ell'} + \delta_{n_1,n_1'}(\mathbf{K}_{R_2,\ell})_{n_2,n_2'}\delta_{\ell,\ell'}. \quad (13)$$

In the last section the two different FBRs, AS-FBR, and S-FBR, were found to yield identical VEs. Therefore, the potential energy matrix is set up using the more advantageous S-FBR resulting in a symmetric representation. Define the $N_1N_2L\times N_1N_2L^2$-dimensional matrix,

$$\mathcal{F}_{n_1'\nu' n_2'\ell', n_1\nu_2 n_2\ell} = w_{n_1}^{1/2} w_{\nu_2 n_2}^{1/2} w_\ell^{1/2} \chi_{n_1'}(r_{n_1}) F_{\nu' n_2'}(r_{\nu_2 n_2}) P_{\ell'}(q_\ell) = \delta_{n_1',n_1} w_{\nu_2 n_2}^{1/2} w_\ell^{1/2} F_{\nu' n_2'}(r_{\nu_2 n_2}) P_{\ell'}(q_\ell). \quad (14)$$

$\boldsymbol{\mathcal{F}}$ is a sparse matrix of special structure, since $\chi_{n_1'}(r_{n_1}) = w_{n_1}^{-1/2}\delta_{n_1',n_1}$, while w_{n_1} and w_ℓ are Gaussian weights, and $w_{\nu_2 n_2}$ were set to one during the computations. One can set up the S-FBR matrix of the Hamilton operator using Eq. (8) and setting $d=1/2$, where in this case **K** is defined in Eq. (13) and $V^{\mathrm{diag}}_{n_1\nu_2 n_2\ell, n_1'\nu_2' n_2'\ell'} = V(r_{n_1}, r_{\nu_2 n_2}, q_\ell)\delta_{n_1\nu_2 n_2\ell, n_1'\nu_2' n_2'\ell'}$. Pictorial representation of the shape of the matrices $\boldsymbol{\mathcal{F}}$ [Eq. (14)], **S** [Eq. (8)], $\mathbf{V}^{\mathrm{FBR}}$ [Eq. (8)], and **H** [Eq. (8)] in the special case of $N_1=3$ and $N_2=4$ is shown in Fig. 1. The Hamiltonian matrix **H** is a symmetric sparse matrix of special structure with $(N_1+N_2L-1)N_1N_2L$ nonzero elements (see Fig. 1). Therefore, one can compute the required eigenvalues of this Hamiltonian matrix using a Lanczos method[43] specialized for sparse matrices. This algorithm is much more efficient than that described in Sec. III: a computation with the same basis size has used only a few minutes of CPU time instead of a couple of days. Note also that we observed no convergence problems during the Lanczos iterations, and the number of the iterations did not depend on the size of the final Hamiltonian matrix [**H** of Eq. (8)]. This fast convergence is very pleasing and is due to the fact that the $R_2=0$ singularity does not degrade the convergence of the Lanczos technique.[12]

The VEs of H_3^+ between 11 000 and 15 000 cm^{-1} above the vibrational ground state, starting with the 36th vibrational eigenvalue, are presented in Table II. Note that the barrier to linearity on the PES of H_3^+ is at about 10 000 cm^{-1}. The VEs have been calculated both by the DVR/FBR algorithm of this section and by the standard DVR technique termed DOPI.[11,12] In Table II and in the forthcoming text the number of basis functions is given as (N_1N_2L), where N_1, N_2, and L denote the number of the R_1-, R_2-, and Θ-dependent functions, respectively.

Only a modest portion of the eigenenergies computed above 11 000 cm^{-1} depend on the proper treatment of the $R_2=0$ singularity. Even for high-lying eigenenergies, e.g., for the pairs $E_{36,37}(E)$ and $E_{66,67}(E)$, where the symmetry characterization is given in parentheses, the DOPI algorithm, with a modest number of basis functions, can yield reasonable, though sometimes not exceedingly accurate VEs. The fast convergence of the eigenenergies obtained using the DVR/FBR algorithm is apparent from the fact that even the use of a modest 20 Bessel-DVR basis functions result in a maximum error of only 5 cm^{-1}, for the pair $E_{62,63}(E)$ and compared to ''accurate'' VEs given in the last column of Table II, among the first 80 vibrational eigenenergies reported. Convergence of the Bessel-DVR VEs is most protracted when the result from a small-basis DOPI and the DVR/FBR treatments deviate substantially, e.g., for the pairs $E_{45,46}(E)$, $E_{48,49}(E)$, $E_{57,58}(E)$, $E_{62,63}(E)$, $E_{71,72}(E)$, and $E_{75,76}(E)$. One of the largest deviation coming from the smallest, (20 20 20), DOPI calculation reported is 260 cm^{-1} for the pair $E_{62,63}(E)$, again compared to accurate VEs given in the last column of Table II. At the same time, for this pair the (20 20 20) DVR/FBR calculation shows a deviation of only 5 cm^{-1}. The extremely slow convergence of E_{62} with the DOPI scheme is noteworthy: the error of 260 cm^{-1} decreases to only 245 cm^{-1} when the basis is increased to (30 30 30), while the same basis size results in an error of 0.5 cm^{-1} when the DVR/FBR scheme is employed. A similar statement holds to all of the pairs mentioned showing the tremendous difficulty of the simple DOPI scheme in dealing with the $R_2=0$ singularity. Obviously, there are intermediate cases between successes and failures of the DOPI scheme. There seems to be no problem in predicting the eigenenergies of A_2 symmetry: all eigenenergies reported, whether treating the $R_2=0$ singularity or not, agree to within 0.1 cm^{-1}. The situation with the A_1-symmetry eigenenergies is less clearcut. In a few cases, e.g., $E_{41}(A_1)$ and $E_{80}(A_1)$, proper treatment of the singularity makes a rather small difference, the largest DOPI and DVR/FBR eigenenergies differ at most by a couple of cm^{-1}, in cases only by 0.01 cm^{-1}. Nevertheless, in other cases, e.g., for $E_{54}(A_1)$ and $E_{68}(A_1)$, the two algorithms result in considerably different eigenenergies. Again, improving the basis set makes the discrepancy smaller, e.g., for $E_{54}(A_1)$ the difference of 407 cm^{-1} obtained with a basis set of (20 20 20) functions decreases to 212 cm^{-1} when the size of the basis is increased to (30 30

TABLE II. All the vibrational eigenenergies of H_3^+, between 11 000 and 15 000 cm^{-1} above the ground vibrational state, in cm^{-1}. The PES of H_3^+ is taken from Ref. 40 with the minimum at $r_e(HH) = 1.649\,99$ bohrs. $m(H) = 1.007\,537\,2u$ is used during all the computations. The number of basis functions is given as $(N_1\,N_2\,L)$, where N_1, N_2, and L denote the number of the R_1-, R_2-, and Θ-dependent functions, respectively. Without symmetry analysis of the wave function or symmetrization of the basis functions no proper symmetry labels can be attached to the degenerate levels; therefore, these labels are omitted here.

		(20 20 20)		(25 25 25)		(30 30 30)		
Number[a]	Symmetry	BESSEL[b]	DOPI[c]	BESSEL[b]	DOPI[c]	BESSEL[b]	DOPI[c]	Accurate[d]
36	E	11 324.81	11 324.81	11 324.76	11 324.76	11 324.74	11 324.74	11 324.74
37	E	11 325.65	11 325.71	11 324.79	11 324.78	11 324.74	11 324.74	11 324.74
38	A_2	11 528.74	11 528.73	11 527.81	11 527.80	11 527.76	11 527.75	11 527.76
39	E	11 657.88	11 654.01	11 656.96	11 653.82	11 656.92	11 654.30	11 656.92
40	E	11 658.18	11 657.85	11 656.98	11 656.96	11 656.93	11 656.92	11 656.93
41	A_1	11 814.44	11 813.97	11 813.88	11 813.62	11 813.86	11 813.65	11 813.87
42	E	12 078.77	12 077.24	12 078.21	12 077.53	12 078.19	12 077.72	12 078.20
43	E	12 079.32	12 079.30	12 078.25	12 078.24	12 078.19	12 078.19	12 078.20
44	A_1	12 149.74	12 146.94	12 149.41	12 149.39	12 149.38	12 149.37	12 149.38
45	E	12 300.88	12 301.13	12 300.49	12 300.48	12 300.46	12 300.46	12 300.46
46	E	12 301.12	12 149.79	12 300.58	12 197.76	12 300.51	12 225.71	12 300.47
47	A_1	12 376.20	12 334.41	12 375.55	12 338.73	12 375.44	12 342.41	12 375.38
48	E	12 374.02	12 474.01	12 473.67	12 473.67	12 473.66	12 473.66	12 473.66
49	E	12 474.57	12 433.12	12 473.88	12 437.94	12 473.75	12 441.78	12 473.67
50	A_1	12 590.89	12 587.93	12 589.85	12 587.67	12 589.80	12 587.98	12 589.80
51	E	12 697.22	12 697.18	12 697.31	12 697.31	12 697.29	12 697.29	12 697.29
52	E	12 698.80	12 684.85	12 697.37	12 689.26	12 697.30	12 691.12	12 697.29
53	A_2	12 833.33	12 833.27	12 832.27	12 832.26	12 832.21	12 832.21	12 832.21
54	A_1	13 289.64	12 882.79	13 288.87	12 992.24	13 288.84	13 076.99	13 288.85
55	E	13 319.50	13 318.29	13 318.40	13 318.17	13 318.35	13 318.25	13 318.35
56	E	13 319.52	13 319.44	13 318.40	13 318.40	13 318.36	13 318.35	13 318.35
57	E	13 391.70	13 290.92	13 390.82	13 291.61	13 390.77	13 292.28	13 390.79
58	E	13 392.36	13 392.31	13 390.97	13 390.81	13 390.88	13 390.76	13 390.82
59	A_1	13 399.89	13 393.69	13 398.62	13 393.94	13 398.49	13 394.02	13 398.41
60	E	13 587.28	13 583.32	13 587.36	13 587.15	13 587.31	13 587.31	13 587.31
61	E	13 588.48	13 588.43	13 587.39	13 587.35	13 587.34	13 588.40	13 587.32
62	E	13 686.43	13 432.24	13 691.61	13 439.69	13 691.62	13 446.99	13 691.62
63	E	13 691.68	13 691.68	13 692.65	13 691.61	13 692.17	13 691.62	13 691.67
64	A_1	13 714.79	13 709.18	13 717.56	13 709.23	13 717.35	13 709.34	13 717.13
65	A_2	13 756.03	13 756.02	13 754.60	13 754.59	13 754.55	13 754.54	13 754.56
66	E	14 056.79	14 056.78	14 056.52	14 055.71	14 056.53	14 055.85	14 056.53
67	E	14 057.87	14 056.89	14 056.58	14 056.57	14 056.53	14 056.53	14 056.53
68	A_1	14 191.60	14 116.99	14 191.04	14 147.07	14 190.97	14 158.10	14 190.93
69	E	14 217.58	14 217.49	14 216.95	14 216.94	14 216.93	14 216.93	14 216.94
70	E	14 219.03	14 196.42	14 217.07	14 202.16	14 216.96	14 205.23	14 216.94
71	E	14 474.00	14 474.90	14 473.56	14 473.55	14 473.49	14 473.49	14 473.50
72	E	14 474.97	14 315.00	14 473.58	14 385.39	14 473.54	14 426.67	14 473.51
73	A_2	14 565.55	14 565.52	14 565.55	14 565.54	14 565.55	14 565.54	14 565.56
74	A_1	14 665.28	14 665.56	14 665.89	14 667.61	14 665.90	14 667.35	14 665.91
75	E	14 880.12	14 880.08	14 879.53	14 879.53	14 879.52	14 879.51	14 879.54
76	E	14 881.00	14 423.87	14 880.29	14 460.92	14 879.86	14 493.08	14 879.56
77	A_1	14 883.81	14 579.18	14 889.90	14 650.76	14 889.81	14 702.72	14 889.71
78	E	14 890.59	14 888.44	14 890.51	14 888.61	14 890.59	14 888.66	14 890.61
79	E	14 890.67	14 890.67	14 890.59	14 890.57	14 890.61	14 890.59	14 890.62
80	A_1	14 943.71	14 942.70	14 943.06	14 942.96	14 943.01	14 942.93	14 943.01

[a]The first 35 eigenvalues, including the zero-point energy, are not reported in this table.

[b]BESSEL, results obtained by the algorithm described in Sec. IV, where the R_1 Hermite-DVR grid points are in the interval [0.9,4.5] and the radial R_2 Bessel grid ponts are $0 < r_{\nu_2 n_2} \leqslant 3.5 + [0.001(\nu_2 + 1/2)]$, all in bohr.

[c]DOPI, results obtained by DOPI, where the R_1 and R_2 Hermite-DVR grid points are in the intervals [0.9,4.5] and [0.05,3.55] bohrs, respectively.

[d]Converged results obtained by a large (35 60 35) BESSEL computation.

30). Two examples concerning the convergence of the computed VEs are given on Fig. 2. The eigenvalue E_{12} is below the barrier and thus both the DOPI and the Bessel-DVR/FBR approaches work well and their convergence characteristic is similar. The eigenvalue E_{46} is above the barrier and the large deviations resulting from not treating the singularity is apparent. Note that the convergence behavior of the DVR/FBR approach is similar for the two eigenvalues.

Using the Hermite-DVR in DOPI one can choose the smallest grid point, $R_2^{\min}$ [see Eq. (12)]. VEs of H_3^+ between

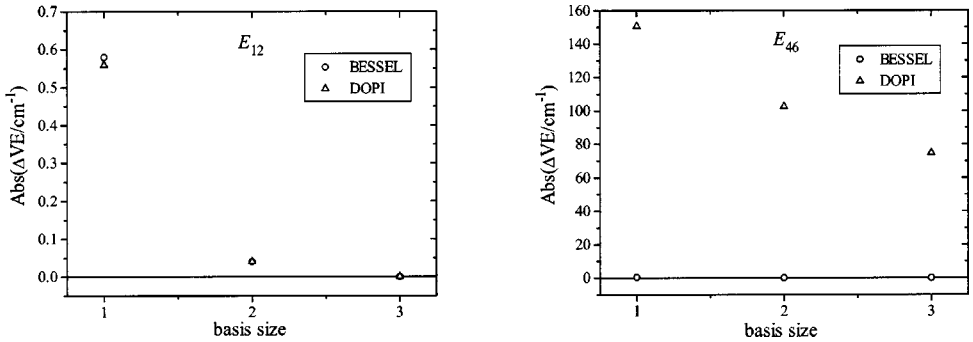

FIG. 2. Dependence of the vibrational eigenvalues E_{12} at 7005.00 cm^{-1} and E_{46} at 12300.46 cm^{-1} of H_3^+ on the size of the basis [basis 1, (20 20 20); basis 2, (25 25 25); and basis 3, (30 30 30)] and the strategy, DOPI vs BESSEL (see Sec. IV), employed for the solution of the Schrödinger equation, where ΔVE is the difference between the actual and the accurate eigenvalues.

11 000 and 13 000 cm^{-1}, obtained by varying $R_2^{\min}$, are presented in Table III. Setting $R_2^{\min}$ to too small of a value, e.g., 0.01 bohr, results in errors in all the computed VEs. This can be explained by the failure of the quadrature approximation when the $R_2=0$ singularity is present. By setting a higher $R_2^{\min}$ value, converged VEs can be calculated when the singularity does not come into play. For example, for the pairs $E_{36,37}(E)$ the same converged VEs were computed by setting $R_2^{\min}$ either to 0.05 or to 0.1. When the singularity comes into play, different $R_2^{\min}$ choices, employing the same basis size, result in different unconverged VEs. For example, for the pairs $E_{45,46}(E)$ setting $R_2^{\min}$ either to 0.05 or to 0.1, the same converged E_{45} was obtained; however, in the case of E_{46}, where the singularity becomes important, the two (30 30 30) calculations result in a discrepancy of more than 30 cm^{-1}.

V. CONCLUSIONS

Appearance of certain singular terms is unavoidable when the (ro)vibrational Hamiltonian is expressed in internal coordinates. Two methods have been developed in this paper to cope with the singular terms of the vibrational kinetic energy operator of a triatomic molecule given in orthogonal internal coordinates, such as Jacobi or Radau coordinates $\{R_1,R_2,\Theta\}$, when solving the related time-independent Schrödinger equation.

The first method, a FBR algorithm, gives a mathematically correct treatment of all singular terms. In this technique the vibrational eigenfunctions are approximated by linear combinations of functions of a three-dimensional nondirect-product basis. These basis functions are formed by coupling

TABLE III. All the vibrational eigenenergies of H_3^+, between 11 000 and 13 000 cm^{-1} above the ground vibrational state, in cm^{-1}, computed by the DOPI algorithm varying the smallest R_2 grid point. In all the cases the R_1 Hermite-DVR grid points are in the interval [0.9,4.5] bohrs. The R_2 Hermite-DVR grid points are in the intervals [0.01,3.59], [0.05,3.55], and [0.1,3.5] bohrs, respectively. The PES of H_3^+ is taken from Ref. 40, and $m(H)=1.007\,537\,2u$ is used during the computations. The number of basis functions is given as $(N_1\,N_2\,L)$, where N_1, N_2, and L denote the number of the R_1-, R_2-, and Θ-dependent functions, respectively.

		(20 20 20)			(25 25 25)			(30 30 30)			
Number	Symmetry	0.01	0.05	0.1	0.01[a]	0.05	0.1	0.01[a]	0.05	0.1	Accurate[b]
36	E	11 325.07	11 324.81	11 324.81	11 324.78	11 324.76	11 324.76	11 325.24	11 324.74	11 324.74	11 324.74
37	E	11 325.45	11 325.71	11 325.71	11 328.51	11 324.78	11 324.78	11 328.29	11 324.74	11 324.74	11 324.74
38	A_2	11 528.71	11 528.73	11 528.73	11 526.80	11 527.80	11 527.80	11 528.62	11 527.75	11 527.75	11 527.76
39	E	11 653.73	11 654.01	11 654.85	11 655.89	11 653.82	11 654.58	11 656.72	11 654.30	11 655.02	11 656.92
40	E	11 657.92	11 657.85	11 657.86	11 658.60	11 656.96	11 656.96	11 674.61	11 656.92	11 656.92	11 656.93
41	A_1	11 814.00	11 813.97	11 814.06	11 812.83	11 813.62	11 813.68	11 816.81	11 813.65	11 813.71	11 813.87
42	E	12 075.61	12 077.24	12 077.97	12 077.14	12 077.53	12 077.81	12 079.58	12 077.72	12 077.90	12 078.20
43	E	12 079.30	12 079.30	12 079.30	12 078.11	12 078.24	12 078.25	12 083.16	12 078.19	12 078.19	12 078.20
44	A_1	12 112.14	12 146.94	12 149.51	12 148.50	12 149.39	12 149.40	12 150.58	12 149.37	12 149.37	12 149.38
45	E	12 301.11	12 301.13	12 301.13	12 300.70	12 300.48	12 300.48	12 303.21	12 300.46	12 300.46	12 300.46
46	E	12 149.42	12 149.79	12 199.69	12 212.75	12 197.76	12 238.26	12 305.33	12 225.71	12 258.31	12 300.47
47	A_1	12 332.56	12 334.41	12 339.03	12 341.87	12 338.73	12 344.71	12 382.71	12 342.41	12 349.60	12 375.38
48	E	12 474.06	12 474.01	12 474.01	12 473.74	12 473.67	12 473.67	12 476.89	12 473.66	12 473.66	12 473.66
49	E	12 430.84	12 433.12	12 438.64	12 441.97	12 437.94	12 444.08	12 478.42	12 441.78	12 448.55	12 473.67
50	A_1	12 586.78	12 587.93	12 588.64	12 591.76	12 587.67	12 588.20	12 590.31	12 587.98	12 588.46	12 589.80
51	E	12 697.03	12 697.18	12 697.20	12 697.88	12 697.31	12 697.31	12 699.52	12 697.29	12 697.29	12 697.29
52	E	12 680.33	12 684.85	12 689.90	12 688.02	12 689.26	12 692.03	12 703.34	12 691.12	12 693.29	12 697.29
53	A_2	12 825.06	12 833.27	12 833.31	12 833.24	12 832.26	12 832.27	12 834.25	12 832.21	12 832.21	12 832.21

[a]The too small R_2 grid point can result in a ghost eigenvalue and small errors in the vibrational eigenenergies.
[b]Converged results taken from Table II.

Bessel-DVR functions[35] depending on distance-type coordinates R_1 and R_2 and Legendre polynomials depending on the angle bending coordinate Θ.

In the Jacobi coordinate system the $R_1=0$ singularity will not occur in physically relevant cases as the potential energy value is going to be infinite and the wave function is going to vanish near nuclear coalescense points, thus it is unimportant for bound vibrational states. A second method is, therefore, formed by not treating the singular term characterized by the Jacobi coordinate R_1. In this case the basis set is obtained by taking the direct product of a standard DVR basis, representing R_1, with a two-dimensional nondirect-product basis, formed by coupling Bessel-DVR functions representing R_2 and Legendre polynomials depending on Θ.

In the first case, given the basis functions detailed above, matrix representations of the time-independent Schrödinger equation are set up and solved numerically to obtain the vibrational energy levels of H_3^+. The matrix elements of the kinetic energy operator are calculated analytically. The matrix elements of the potential energy operator are calculated by numerical quadrature. Two different prescriptions of numerical integration corresponding to two special cases of the finite basis representation related to the generalized discrete variable representation[6] are employed. The theoretically more accurate scheme gives an asymmetrical FBR, whereas another treatment,[2] gives a symmetrical FBR. With the grid points employed the symmetric and the asymmetric FBRs give extremely similar results for all vibrational eigenenergies irrespective of the basis size. This suggests that the quadrature points chosen may be close to optimal though their number is perhaps larger than needed. It is our intent to revisit the use of quadrature points and find a numerically more easily managable set of quadrature points which still allows an efficient calculation of the potential matrix elements.

The numerical calculations performed for H_3^+, employing a published[40] potential energy surface, have shown that the first method, treating all singularities properly, requires a large amount of CPU time for the construction of the potential energy matrix and is thus computationally inefficient. The second method, treating properly only the physically relevant singularities, is quite efficient. Using the more advantageous S-FBR to set up a symmetric potential energy matrix the Hamiltonian matrix becomes a symmetric sparse matrix of special structure with $(N_1+N_2L-1)N_1N_2L$ nonzero elements. The desired number of converged energy eigenstates has been computed by an iterative Lanczos algorithm.

A standard DVR technique termed DOPI (Refs. 11 and 12) has also been used to compute the vibrational eigenenergies of H_3^+ employing the same PES. Comparison of the DVR/FBR eigenvalues with those calculated by the DOPI scheme, which employs basis functions inappropriate for handling the singular terms in question, clearly demonstrates the effect and importance of a proper treatment of singular terms in the case of H_3^+.

It seems[44] certainly appealing to employ the treatment presented in this paper based on Bessel functions for computing resonances of H_3^+, and this will be investigated in the near future.

ACKNOWLEDGMENTS

The work described received a small amount of support from the Hungarian Scientific Research Fund, OTKA, through Grant Nos. T047185 and T045955. Discussions with Professor Jonathan Tennyson (UCL, London) on the topic of this paper, helped by an INTAS Grant No. 03-51-3394, are gratefully acknowledged. The authors are also thankful to Professor Tennyson and Jayesh Ramanlal for supplying them with a FORTRAN subroutine containing the PES of H_3^+ of Ref. 40 employed in all the calculations. The authors thank Professor Brian Sutcliffe and Professor Tucker Carrington, Jr., for their comments concerning the manuscript. Discussions with Zoltán Kurucz are also gratefully acknowledged.

[1] See, for example, Special Issue of Spectrochim. Acta, Part A **58A**, (2002).
[2] J. C. Light, I. P. Hamilton, and J. V. Lill, J. Chem. Phys. **82**, 1400 (1985).
[3] D. O. Harris, G. G. Engerholm, and W. D. Gwinn, J. Chem. Phys. **43**, 1515 (1965).
[4] A. S. Dickinson and P. R. Certain, J. Chem. Phys. **49**, 4209 (1968).
[5] V. Szalay, G. Czakó, A. Nagy, T. Furtenbacher, and A. G. Császár, J. Chem. Phys. **119**, 10512 (2003).
[6] J. C. Light and T. Carrington, Jr., Adv. Chem. Phys. **114**, 263 (2000).
[7] V. Szalay, J. Chem. Phys. **105**, 6940 (1996).
[8] J. R. Henderson and J. Tennyson, Comput. Phys. Commun. **75**, 365 (1993).
[9] J. Tennyson, M. A. Kostin, P. Barletta, G. J. Harris, O. L. Polyansky, J. Ramanlal, and N. F. Zobov, Comp. Phys. Comm. (to be published).
[10] B. T. Sutcliffe and J. Tennyson, Int. J. Quantum Chem. **39**, 183 (1991).
[11] G. Czakó, T. Furtenbacher, A. G. Császár, and V. Szalay, Mol. Phys. **102**, 2411 (2004).
[12] M. J. Bramley and T. Carrington, Jr., J. Chem. Phys. **99**, 8519 (1993).
[13] I. N. Kozin, M. N. Law, J. M. Hutson, and J. Tennyson, J. Chem. Phys. **118**, 4896 (2002).
[14] M. J. Bramley and N. C. Handy, J. Chem. Phys. **98**, 1378 (1993); S. Carter, N. Pinnavaia, and N. C. Handy, Chem. Phys. Lett. **240**, 400 (1995).
[15] D. Luckhaus, J. Chem. Phys. **118**, 8797 (2003).
[16] M. Mladenović, Spectrochim. Acta, Part A **58A**, 795 (2002).
[17] H.-G. Yu, J. Chem. Phys. **117**, 2030 (2002).
[18] X.-G. Wang and T. Carrington, Jr., J. Chem. Phys. **119**, 101 (2003).
[19] X.-G. Wang and T. Carrington, Jr., J. Chem. Phys. **121**, 2937 (2004).
[20] H.-G. Yu, J. Chem. Phys. **120**, 2270 (2003).
[21] B. T. Sutcliffe, J. Chem. Soc., Faraday Trans. **89**, 2321 (1993).
[22] J. L. Gottfried, B. J. McCall, and T. Oka, J. Chem. Phys. **118**, 10890 (2003).
[23] A. V. Meremianin and J. S. Briggs, Phys. Rep. **384**, 121 (2003).
[24] For example, for triatomic vibrational calculations in hyperspherical coordinates, used by S. Carter and W. Meyer, J. Chem. Phys. **93**, 8902 (1990) and others, no radial singularity is present in the Hamiltonian. Recently the approach using hyperspherical coordinates has been extended to obtain eigenstates beyond the barrier to linearity by P. Schiffels, A. Alijah, and J. Hinze, Mol. Phys. **101**, 189 (2003).
[25] H. Wei and T. Carrington, Jr., J. Chem. Phys. **101**, 1343 (1994).
[26] V. Spirko, A. Cejhan, and P. Jensen, J. Mol. Spectrosc. **134**, 430 (1987).
[27] J. R. Henderson, J. Tennyson, and B. T. Sutcliffe, J. Chem. Phys. **98**, 7191 (1993).
[28] J. Tennyson and B. T. Sutcliffe, J. Mol. Spectrosc. **101**, 71 (1983).
[29] J. K. G. Watson, Can. J. Phys. **72**, 702 (1994); J. K. G. Watson, Chem. Phys. **190**, 291 (1995).
[30] M. J. Bramley, J. W. Tromp, T. Carrington, Jr., and G. C. Corey, J. Chem. Phys. **100**, 6175 (1994).
[31] For vibration-only calculations the spherical oscillator and the spherical harmonic oscillator functions are identical.
[32] V. A. Mandelshtam and H. S. Taylor, J. Chem. Soc., Faraday Trans. **93**, 847 (1997).
[33] M. Vincke, L. Malegat, and D. Baye, J. Phys. B **26**, 811 (1993).
[34] M. Hesse, Phys. Rev. E **65**, 046703 (2002).

[35] R. G. Littlejohn and M. Cargo, J. Chem. Phys. **117**, 27 (2002).
[36] D. Lemoine, J. Chem. Phys. **118**, 6697 (2003).
[37] C. G. J. Jacobi, Cr. Hebd. Acad. Sci. **15**, 236 (1842).
[38] R. Radau, Ann. Sci. Ec. Normale Super. **5**, 311 (1868).
[39] V. Szalay, J. Chem. Phys. **99**, 1978 (1993).
[40] O. L. Polyansky, R. Prosmiti, W. Klopper, and J. Tennyson, Mol. Phys. **98**, 261 (2000).
[41] The imaginary part of the vibrational eigenenergies obtained from the AS-FBR representation turned out to be zero for all the eigenvalues investigated.
[42] Almost all of the CPU time is spent in building a matrix representation of the potential energy operator, explicit diagonalization of the final Hamiltonian took a trivial amount of computer time.
[43] J. K. Cullum and R. A. Willoughby, *Lanczos Algorithms for Large Symmetric Eigenvalue Computations* (SIAM, Philadelphia, 2002).
[44] J. Tennyson (private communication).